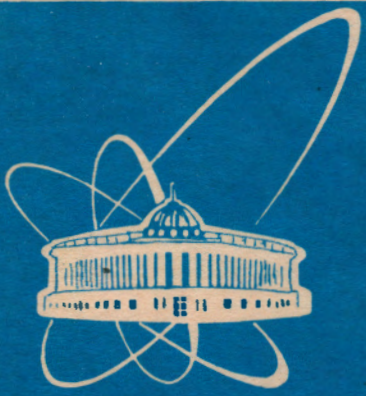

ОБЪЕДИНЕННЫЙ
ИНСТИТУТ
ЯДЕРНЫХ
ИССЛЕДОВАНИЙ

Дубна

96-45

E1-96-45

A.G.Olchevski

PRECISION TESTS OF THE STANDARD MODEL

Invited talk given at the 1995 International Europhysics Conference on High-Energy Physics, Brussels, Belgium

1996

1 Introduction

The high accuracy of present electroweak measurements make them sensitive to the level of quantum corrections in the Standard Model (SM) of electroweak interactions.

Different electroweak measurements complement each other in their sensitivity to the Standard Model parameters. By confronting these measurements to the theory predictions one can check the internal consistency of the Standard Model and extract the information on the SM parameters.

The SM predictions for electroweak observables are usually made in terms of:

experimentally well measured quantities - the mass of the Z^0, M_Z, the muon decay constant, G_μ, the fine structure constant at M_Z-scale, $\alpha(M_Z^2)$;

and less known - the strong coupling constant at M_Z-scale, $\alpha_s(M_Z^2)$, the mass of the top-quark, m_t, and the Higgs boson mass, M_H.

The value of $\alpha_s(M_Z^2)$ is measured now at LEP to about 5% precision.

Top-quark has been discovered recently at the TEVATRON and its mass was measured directly to a precision of $\sim$ 12 GeV. This direct measurement is in excellent agreement with the m_t prediction from radiative corrections, to which many of recent precise electroweak measurements performed at LEP, SLC, TEVATRON, as well as some others, had contributed to.

With the direct measurement of m_t the electroweak data already show weak sensitivity to M_H, the most unknown and intriguing parameter.

In the subsequent sections the results of the most precise measurements of the W and Z^0 masses, the widths and various lepton and quark asymmetries are presented. Finally, the results of the global analysis of the electroweak data are discussed.

2 Z^0 lineshape results

2.1 Definition of the parameters

The, so-called, Z^0 lineshape is the measurement of the cross sections of the production of different fermions at several energy points around the resonance. From these measurements the basic parameters of the Z^0 - the mass, the total and the partial widths are extracted.

At the energies near the Z^0 resonance the total cross section for the process $e^+e^- \to f\bar{f}$ with $f \neq e$ is dominated by Z^0 exchange. In the lowest order it can be written as:

$$\sigma_{f\bar{f}}(s) = \sigma^0_{f\bar{f}} \frac{s\Gamma_Z{}^2}{(s - M_Z{}^2)^2 + (M_Z\Gamma_Z)^2} + \gamma Z^0 + \gamma, \qquad (1)$$

where 'γ' and 'γZ^0' are small contributions from the photon exchange and the γZ^0-interference. The peak cross section $\sigma^0_{f\bar{f}}$ can be expressed through the total and partial widths of the Z^0:

$$\sigma^0_{f\bar{f}} = 12\pi \frac{\Gamma_{ee}\Gamma_{f\bar{f}}}{M_Z{}^2\Gamma_Z{}^2}, \qquad (2)$$

and partial widths are proportional to the combination of the Z^0 vector and axial-vector couplings to the fermions:

$$\Gamma_{f\bar{f}} \sim (g_v^{f\,2} + g_a^{f\,2}). \qquad (3)$$

Another combination of these couplings, namely the ratio g_v^f / g_a^f, is measured from the forward-backward asymmetries.

In the Standard Model the polar angular dependence of the cross section for the process $e^+e^- \to f\bar{f}$ (f$\neq$e) is given by:

$$\frac{d\sigma(s)}{d\cos\theta} \sim 1 + \cos^2\theta + \frac{8}{3} A_{FB}(s) \cos\theta, \qquad (4)$$

where θ is an angle between the directions of the incoming e^+ and the outgoing antifermion $\bar{f}$. For f=e a more complicated expression arises from the t-channel involved. Parameter $A_{FB}(s)$ is the forward-backward (FB) asymmetry defined as:

$$A_{FB}(s) = \frac{\sigma_F(s) - \sigma_B(s)}{\sigma_F(s) + \sigma_B(s)}. \qquad (5)$$

The experimental information about FB asymmetry is often expressed in a single number, so-called, peak asymmetry $A_{FB}^{0,f}$ defined as:

$$A_{FB}^{0,f} \equiv A_{FB}^f(s = M_Z^2) = \frac{3}{4} \mathcal{A}_e \mathcal{A}_f, \qquad (6)$$

with

$$\mathcal{A}_f = \frac{2\, g_v^f\, g_a^f}{g_v^{f\,2} + g_a^{f\,2}}. \qquad (7)$$

The weak mixing angle is defined as the ratio of the vector and axial-vector coupling constants of the fermion to Z^0.

$$\sin^2\theta_W^{eff,f} \equiv \frac{1}{4}(1 - g_v^f / g_a^f). \qquad (8)$$

Thus, the measurement of the forward-backward asymmetry provides very important information on the value of $\sin^2\theta_W^{eff}$, which is complementary to the information from the Z^0 lineshape data.

2.2 The data analyses

One can distinguish several important ingredients of the lineshape measurements:

- centre-of-mass energy
- luminosity
- selection of Z^0-events

Significant progress has been achieved in the calibration of the LEP energy using the resonance depolarization technique. This method is a very powerful tool with an internal precision of a fractions of MeV in a single energy measurement. A series of calibrations of LEP were performed in 1993 when LEP was taking data at peak-2, peak and peak+2 energies.

Analysis of these data along with the information on many parameters of LEP which were monitored during this scan allowed to calibrate energy points to a 2.0, 5.4 and 1.5 MeV, respectively [1]. Taking into account the correlation between the calibration of energy points and the weight of '93 data in the whole data set, that resulted in the systematic uncertainties of 1.5 MeV on M_Z and 1.7 MeV on Γ_Z. Additional systematic error of 1.0 MeV on Γ_Z arises from the 5 MeV uncertainty of the LEP centre-of-mass energy spread.

The luminosity provided by LEP was constantly increasing from year to year. During the 1993 scan about 40 pb^{-1} were delivered by LEP to each experiment. This luminosity was approximately equally shared between the peak and off-peak energy points. In 1994 more than 60 pb^{-1} were provided by LEP at peak energy.

The precise determination of the luminosity in each experiment is based on the use of small-angle Bhabha scattering ($e^+e^- \to e^+e^-$) as a reference process. The absolute luminosity is obtained from the ratio of the measured number of events and the theoretically predicted cross-section visible in the acceptance of the Small Angle Taggers (SAT).

Due to a very sharp angular dependence of the Bhabha cross section at small angles the uncertainty on the inner edge of the acceptance represents the major experimental uncertainty in luminosity determination. Overall experimental uncertainties in luminosity analysis of different LEP experiments ranges from 0.08 to 0.15% now.

In addition, there is a theoretical systematic error [2] of 0.16% mainly due to uncalculated higher order terms. This error is treated as common for all experiments. Hopefully, with the new calculations it can be reduced further to match experimental achievement.

The selection of Z^0 events is based on the criteria of energy deposited in the detector and the multiplicity of particles in the event. Lineshape analyses are performed separately for electrons, muons and taus, and for hadrons inclusively.

The hadronic Z^0 decays are separated on the basis of large multiplicity of tracks or calorimetric clusters and require some minimum amount of energy to reject residual background from beam gas events and two-photon interactions. Systematic uncertainties on the selection of Z^0 hadronic events by different LEP experiments are about 0.1% at present.

Leptonic events have low multiplicities and, in addition, the detector particle identification capabilities are used to distinguish between the different lepton types. At present leptonic analyses are still statistically limited, typical experimental systematic uncertainties are 0.3-0.8 %.

The statistics of the Z^0 events collected by the LEP experiments [3] are shown in table 1. In total, from 1990 to 1994, about 12 million hadronic and 1.3 million leptonic decays of Z^0 were detected. The analyses of 1993-1994 data are preliminary.

Table 1: Statistics of the LEP experiments expressed in units 10^3.

		ALEPH	DELPHI	L3	OPAL
$q\bar{q}$	'90-'91	451	356	416	454
	'92	680	697	678	733
	'93 prel.	640	677	654	646
	'94 prel.	1281	1144	1362	1524
	total	3052	2874	3110	3357
$\ell^+\ell^-$	'90-'91	55	37	40	58
	'92	82	69	58	88
	'93 prel.	78	71	61	82
	'94 prel.	155	54	123	184
	total	370	231	282	412

In addition to the total cross section measurement, the angular dependence of the lepton cross section provides an important information on the forward-backward asymmetry.

Experimentally the forward-backward asymmetry is determined by fitting the angular distribution of events at each energy point. In the case of the e^+e^- final state, the calculated t-channel contribution is accounted for.

In the measurement of the ratio of the cross sections many detector systematics cancel out, therefore, the asymmetry measurement is robust. These measurements are still statistically dominated, typical experimental systematics on the analyses of lepton forward-backward asymmetries are 0.001-0.003. Small common systematic error of 0.0005 between different experiments is due to the uncertainty in the absolute LEP energy scale.

2.3 Averaging procedure and results

In order to simplify the comparison and averaging of the lineshape and asymmetry results each LEP experiment provides them in the agreed form of 9-parameters. These parameters are: the Z^0 mass (M_Z), the total width (Γ_Z), the peak hadronic cross-section (σ^0_h), the ratios of the hadronic to leptonic partial widths (R_e, R_μ, R_τ) and leptonic peak asymmetries ($A^{0,e}_{FB}$, $A^{0,\mu}_{FB}$, $A^{0,\tau}_{FB}$). This set is convenient for fitting and averaging as it is the least correlated parameter set close to the experimental measurements.

In the framework of the hypothesis of lepton universality this set is reduced to the 5-parameter set, namely, M_Z, Γ_Z, σ^0_h, R_ℓ and $A^{0,\ell}_{FB}$.

To extract the parameters the cross-sections and asymmetries measured at different energy points are fitted to the theoretical calculations and then the individual experiment results are averaged taking into account common errors and correlations between the parameters [3]. The following common systematic errors were taken

into account in this analysis:

Table 2: Summary of common systematic uncertainties

parameter	uncertainty	source
M_Z	1.5 MeV	LEP energy scale
Γ_Z	1.7 MeV	LEP energy scale
	1.0 MeV	LEP energy spread
σ_h^0	0.16%	Luminosity theory
$A_{FB}^{0,e}$, $A_{FB}^{0,\mu}$, $A_{FB}^{0,\tau}$ or $A_{FB}^{0,\ell}$	0.0005	LEP energy scale

The results of the M_Z measurement by different LEP experiments and their average are shown in figure 1. The errors quoted for the individual LEP experiments are only statistical. Combined result includes common systematics. The mass of the Z^0 is one of the most precisely measured electroweak parameters.

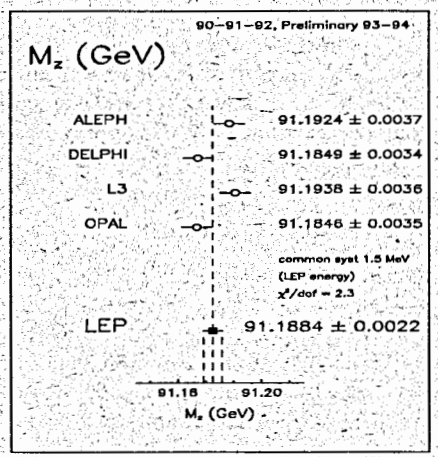

Figure 1: M_Z measurement.

The individual measurements of the Γ_Z, σ_h^0, R_ℓ and $A_{FB}^{0,\ell}$ and their averages are presented in figures 2 - 5. Also shown in these figures are the Standard-Model predictions for different top-quark masses and the range of M_H and $\alpha_s(M_Z^2)$.

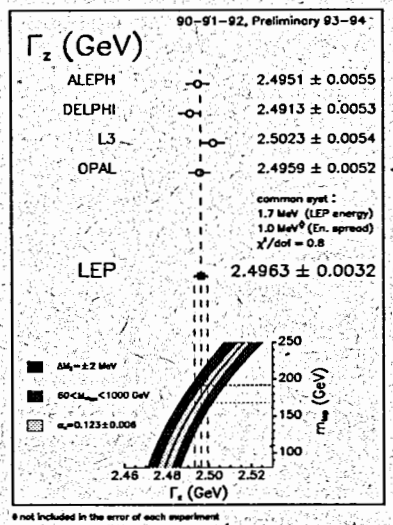

Figure 2: Γ_Z measurement.

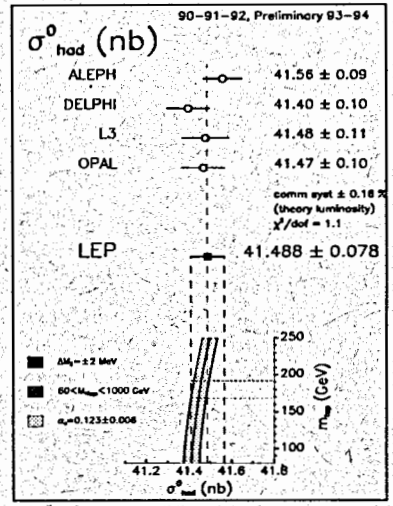

Figure 3: σ_h^0 measurement.

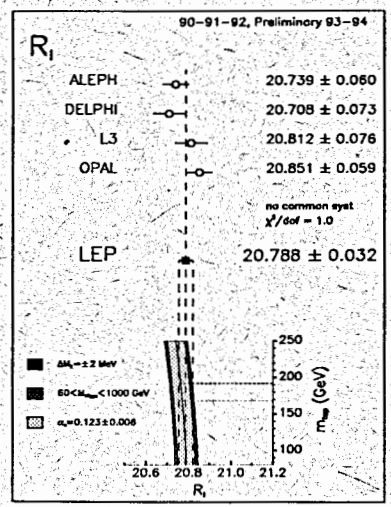

Figure 4: R_ℓ measurement.

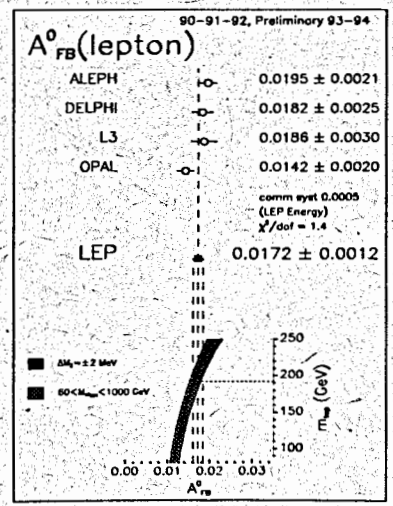

Figure 5: $A_{FB}^{0,\ell}$ measurement.

The Γ_Z dependence on m_t is strong compared to the measurement precision. The total width, therefore, provides an important information for constraining the Standard Model.

The hadronic peak cross-section and the ratio of the hadronic to leptonic Z^0 partial widths, on the contrary, depend only weakly on the parameters m_t and M_H because of the cancellation of similar dependences in partial and total widths. In σ_h^0 the dependence on $\alpha_s(M_Z^2)$ also cancels out partially between Γ_{had} and Γ_Z^2. However, the dependence of R_ℓ on $\alpha_s(M_Z^2)$ is strong, which makes R_ℓ the most important observable for the extraction of the strong coupling constant from the Z^0 line shape data.

Figure 6 shows the correlation between the measured ratios of hadronic to leptonic partial widths and peak asymmetries for different lepton species and for all leptons assuming universality.

Table 3: Average lineshape and lepton forward-backward asymmetry results.

M_Z(GeV)	91.1884±0.0022
Γ_Z(GeV)	2.4963±0.0032
σ_h^0(nb)	41.488±0.078
With Lepton Universality	
R_ℓ	20.788±0.032
$A_{FB}^{0,\ell}$	0.0172±0.0012
Without Lepton Universality	
R_e	20.797±0.058
R_μ	20.796±0.043
R_τ	20.813±0.061
$A_{FB}^{0,e}$	0.0157±0.0028
$A_{FB}^{0,\mu}$	0.0163±0.0016
$A_{FB}^{0,\tau}$	0.0206±0.0023

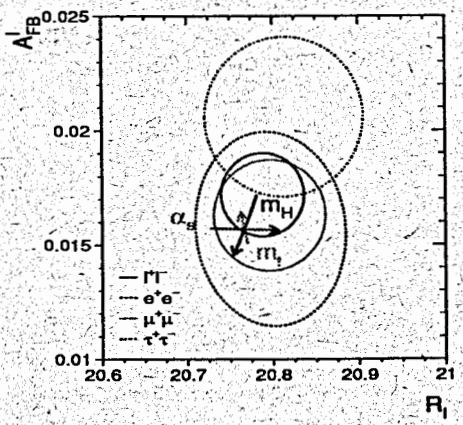

Figure 6: Contour plot for R_ℓ and $A_{FB}^{0,\ell}$ measurement.

Table 4: Average values of the derived parameters.

Γ_{ee}(MeV)	83.92±0.17
$\Gamma_{\mu\mu}$(MeV)	83.92±0.23
$\Gamma_{\tau\tau}$(MeV)	83.85±0.29
Γ_l(MeV)	83.93±0.14
Γ_{had}(MeV)	1744.8±3.0
Γ_{inv}(MeV)	499.9±2.5

Combined between experiments lineshape and asymmetry results with and without assuming lepton universality are summarized in table 3. In addition, in table 4 the lineshape data are presented in the form of partial decay widths of the Z^0 calculated from the parameters of table 3 and correlations.

The measured value of Γ_{inv}/Γ_l=5.956±0.031 corresponds to the number of light neutrino species:

$$N_\nu = 2.991 \pm 0.016\,, \tag{9}$$

when using the Standard Model prediction for one generation Γ_ν/Γ_{ll}=1.991±0.001 computed for M_Z=91.1884 GeV, m_t=180±12 GeV and a variation of M_H from 60 to 1000 with the central value of 300 GeV.

2.4 Study of the γZ^0 interference

The results presented above are different parameterizations of pure Z^0 exchange. In extracting them from the data the common approach of LEP experiments was to fix the small contributions of pure photon exchange and γZ^0 interference to the values predicted by the Standard Model. This is well motivated by the small contribution of these terms at Z^0 energies.

A more general approach, however, is to parameterize the γZ^0 interference independently on the Z^0 exchange and try to extract information on the interference strength from the data [4]. A convenient framework for that is the s-matrix approach in which the total cross section of $e^+e^- \to f\bar{f}$ depend upon the parameters g_f^{tot}, r_f^{tot}, j_f^{tot} - the γ, the Z^0 and the interference contributions, respectively.

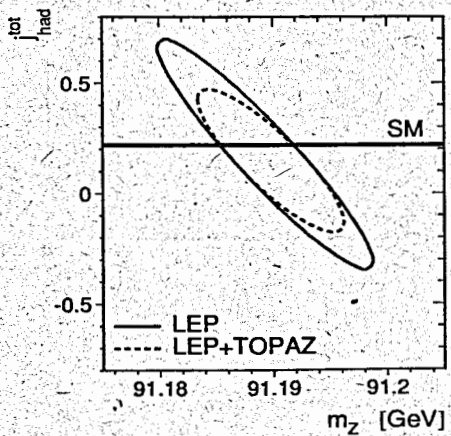

Figure 7: The 68% probability contours for the mass of the Z^0 and the hadronic γZ^0 interference term for the total cross section.

The parameter j^{tot}_{had}, which characterize the hadronic interference term, is strongly correlated with the mass of Z^0. This is shown in figure 7 for combined LEP data and for the data which include the TOPAZ-experiment results.

One notices that the data at lower energy help to constrain the hadronic interference term better than by LEP alone. The precision is poor at present, anyway. To improve it the measurements at the energies below (or above) Z^0, where the interference contribution is relatively more important, are required.

At LEP the lower energies also could be probed studying the events with the initial state radiation. The results of such analysis performed by DELPHI and L3 [5] for the muon channel are presented in figure 8.

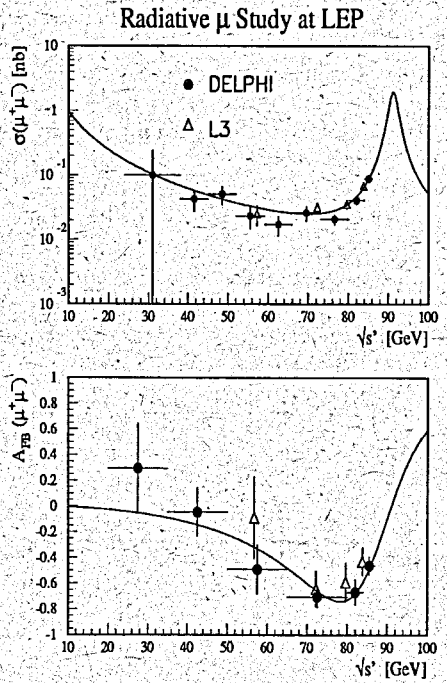

Figure 8: The cross section and forward-backward asymmetry measurement from radiative muon events. The line is the Standard Model expectation.

In this figure the cross section and the forward-backward asymmetry are shown as a function of energy which in these events effectively had changed from the nominal due to the initial state radiated hard photon. Within the limits of precision the data show no deviation from the behaviour predicted by the Standard Model (the line).

3 . τ Polarization

The fermions in the Z^0 decays are produced polarized and in the case of the decay into τ-lepton pair this polarization could be measured experimentally from the analysis of the τ decay properties.

The τ polarization $\mathcal{P}_\tau$ is defined as:

$$\mathcal{P}_\tau = \frac{\sigma_R - \sigma_L}{\sigma_R + \sigma_L} \tag{10}$$

where σ_R and σ_L are the cross-sections for the production of a right-handed and left-handed τ^-, respectively.

Neglecting small corrections, the angular distribution of $\mathcal{P}_\tau(s=M_Z^2)$ is given by:

$$\mathcal{P}_\tau(\cos\theta) = -\frac{\mathcal{A}_\tau + \mathcal{A}_e \frac{2\cos\theta}{1+\cos^2\theta}}{1 + \mathcal{A}_\tau \mathcal{A}_e \frac{2\cos\theta}{1+\cos^2\theta}} \tag{11}$$

where θ is τ production angle (between the e^- and the τ^-), and $\mathcal{A}_e$ and $\mathcal{A}_\tau$ were defined in eqn. (7).

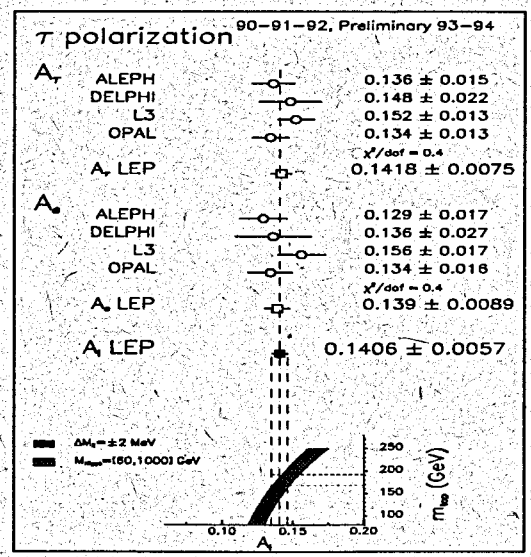

Figure 9: τ-polarization results

Mean τ-polarization (i.e., averaged over all production angles) is the measurement of $\mathcal{A}_\tau$, while as a function of $\cos\theta$, $\mathcal{P}_\tau(\cos\theta)$ provides both $\mathcal{A}_\tau$ and $\mathcal{A}_e$ thus allowing to test lepton universality.

For the τ-polarization measurement LEP experiments use τ decay channels into e, μ, π, ρ and a_1. The DELPHI experiment performed also an inclusive analysis using τ hadronic decays.

The results of individual experiments and their averages [3] for $\mathcal{A}_\tau$, $\mathcal{A}_e$ and a universal $\mathcal{A}_\ell$ are presented in figure 9. The Standard Model prediction shown at the bottom of the figure illustrates the sensitivity of this measurement to the electroweak parameters.

4 The Left-Right asymmetry

The new preliminary result on the left-right asymmetry from the analysis of the SLD data collected up to 1995 was presented recently [6].

Experimentally the left-right asymmetry is measured as a relative difference in the number of Z^0's produced in the collisions of the left- and right-handed electrons with positrons.

$$A_{LR} = \frac{N_L - N_R}{N_L + N_R} = \mathcal{P}_| \mathcal{A}_e \qquad (12)$$

This measurement provides a direct access to the electron couplings to the Z^0. It takes an advantage of the very high ($\sim 80\%$) value of the longitudinal polarization of electron beam, $\mathcal{P}_|$, achieved at SLAC with the strained GaAs polarized electron source.

Two basic aspects of the left-right asymmetry analysis are:

- the measurement of the beam polarization
- the Z^0 counting

The direction of the beam polarization was alternated during the run on a random basis from bunch to bunch to avoid possible biases . The level of the beam polarization was measured in the Compton scattering polarimeter situated after the interaction point. Accurate beam polarization measurements were available approximately every 10 minutes.

The polarization of electron beam versus the integrated statistics of Z^0's collected by SLD is shown in figure 10.

SLD analysis reports an overall relative systematic error of the polarization measurement of 0.8%.

Selection of Z^0 events is performed by SLD experiment on the basis of purely calorimetric information. For this measurement all final states could be analyzed inclusively (in practice, however, the e^+e^- final state is rejected because of the additional t-channel contribution). The selected sample contains 51446 left- and 40815 right-handed Z^0's.

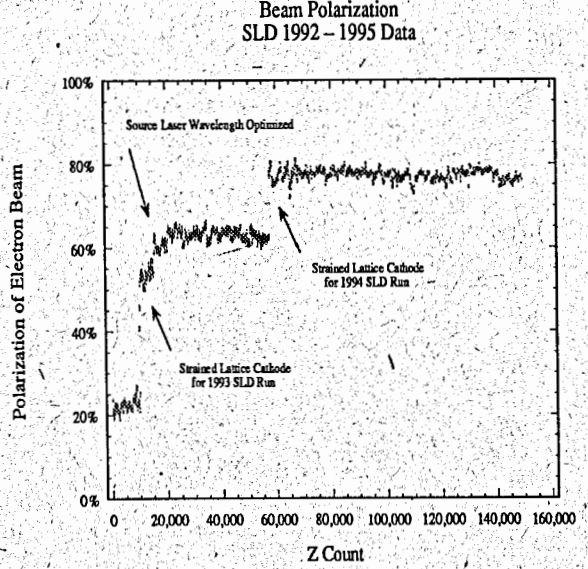

Figure 10: Measured beam polarization.

The new result reads: $\mathcal{A}_e = 0.1524 \pm 0.0042_{stat.} \pm 0.0012_{syst.}$. Including all the SLD data collected from 1992 to 1995 the results is:

$$\mathcal{A}_e = 0.1551 \pm 0.0040 \qquad (13)$$

or expressed in terms of the effective weak mixing angle:

$$\sin^2\theta_W^{eff} = 0.23049 \pm 0.00050 \qquad (14)$$

5 Effective Z^0 couplings for leptons

The data presented above, namely, the partial widths, the lepton forward-backward asymmetries, the τ-polarization, the τ-polarization asymmetry and the left-right asymmetry could be analyzed together to extract information on Z-couplings to charged leptons.

Figure 11 shows the 68% contour plots in the g_a^ℓ-g_v^ℓ plane derived from LEP data. The band in this figure represents the SLD A_{LR} measurement. The Standard Model prediction for m_t=180±12 GeV and a variation of M_H from 60 to 1000 with the central value of 300 GeV is also shown.

The results of the combined LEP+SLD analysis are presented in table 5. The measured ratios of the e, μ and τ couplings given in this table provide a test of the lepton universality. The neutrino couplings to Z^0 were derived from the measured invisible width assuming $g_a^\nu = g_v^\nu = g^\nu$ and the universality of three generations.

Table 5: Results for the effective lepton couplings from the analysis of LEP+SLD data.

Without lepton universality	
g_v^e	-0.03850±0.00087
g_v^μ	-0.0354±0.0036
g_v^τ	-0.0369±0.0018
g_a^e	-0.50103±0.00051
g_a^μ	-0.50124±0.00075
g_a^τ	-0.50152±0.00089
g_a^μ / g_a^e	1.0004±0.0018
g_a^τ / g_a^e	1.0010±0.0020
g_v^μ / g_v^e	0.92±0.10
g_v^τ / g_v^e	0.959±0.052
With lepton universality	
g_v^ℓ	-0.03797±0.00071
g_a^ℓ	-0.50111±0.00041
g^ν	0.5011±0.0013

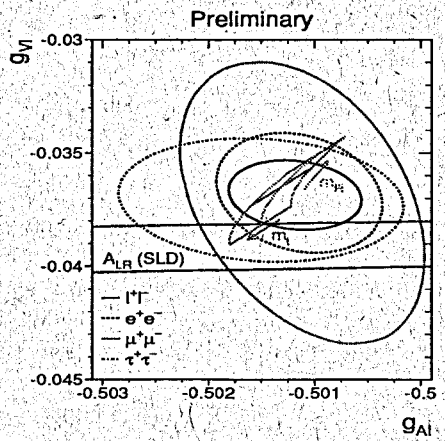

Figure 11: The 68% probability contours in the (g_v^ℓ, g_a^ℓ) plane from LEP and SLC measurements.

6 Electroweak measurements with quarks

6.1 The hadronic charge asymmetry

An inclusive hadronic forward-backward charge asymmetry was measured at LEP by ALEPH, DELPHI and OPAL.

In these analyses the mean difference in jet charges in the forward and backward event hemispheres, $\langle Q_{FB} \rangle$, is related to the original quark forward-backward asymmetries. It is sensitive to the $\sin^2\theta^{lept}_{eff}$ through $\mathcal{A}_e$.

The results on $\langle Q_{FB} \rangle$ from different experiments cannot be compared directly as they include detector dependent effects, so, the comparison and combination of the individual results is performed using the $\sin^2\theta^{lept}_{eff}$ derived by each experiment from the measured hadronic charge asymmetries.

The results of individual experiments and their average [7] are presented in table 6. The dominant systematic error originates from the uncertainties in modelling the fragmentation process.

Table 6: Results on $\sin^2\theta^{lept}_{eff}$ from the measurements of the hadronic charge asymmetries at LEP.

	data	$\sin^2\theta^{lept}_{eff}$
ALEPH	90-93 prel.	$0.2323 \pm 0.0010 \pm 0.0010$
DELPHI	90-91 final	$0.2345 \pm 0.0030 \pm 0.0027$
OPAL	91-94 prel.	$0.2326 \pm 0.0012 \pm 0.0013$
Average		0.2325 ± 0.0013

6.2 Results from b- and c-quarks

The measurements of partial widths and forward-backward asymmetries for b- and c-quarks were performed by ALEPH, DELPHI, L3 and OPAL at LEP [8, 9, 10]. The SLD experiment at SLC has presented recently the measurement of the b-quark partial width and b- and c-quark polarized forward-backward asymmetries [11, 12].

The experimentally measured quantities, R_b and R_c, are the ratios of the b- and c-quark partial widths of the Z^0 to the total hadronic partial width.

These ratios depend rather weakly on the parameters m_t and M_H because of the cancelation of the vacuum polarization corrections in the $\Gamma_{b\bar{b}}$, $\Gamma_{c\bar{c}}$ and Γ_{had}.

In the R_b, however, there is a unique dependence on m_t arising from the b-vertex:

$$R_b \simeq R_q(1 - \frac{20\alpha}{13\pi}(\frac{m_t^2}{M_Z^2} + \frac{13}{6} log \frac{m_t^2}{M_Z^2})) \qquad (15)$$

As in the case of leptons, the quark forward-backward asymmetries are defined by formula (6). With respect to $\mathcal{A}_e$, $\mathcal{A}_q$ is large ($\simeq$0.66 for up and $\simeq$0.93 for down

type quarks) and depends only weakly on $\sin^2\theta_W^{eff}$. The main sensitivity of the quark forward-backward asymmetries is on $\sin^2\theta_W^{eff,\ell}$ through $\mathcal{A}_e$.

The left-right forward-backward asymmetries for b- and c-quarks measured by SLD in the polarized beam are only sensitive to the final state couplings $\mathcal{A}_b$ and $\mathcal{A}_c$ defined in 7.

The exclusive measurements of partial widths in the quark sector require quark flavour tagging. In addition, charge tagging is needed for the asymmetry analysis.

Several methods are used to identify heavy flavour b- and c-quark final states. The tagging techniques are based on: the long lifetime of b-hadrons, special event shapes, which are due to high mass and high momentum of b- and c-hadrons, inclusive leptons with high momentum and high p_T from b- and c-quark decays and a reconstruction of exclusive decay modes.

The measurements performed by experiments could be subdivided into two basic categories: single- and double-tag ones.

In the single-tag technique the number of the identified events is corrected for the background and efficiency calculated using the Monte Carlo. The main systematics of these measurements come from the uncertainties in simulating the production and decay properties of b- and c-hadrons which influence the overall tagging efficiency.

The second class of measurements uses the double-tag technique in which the tagging efficiency is calculated directly from the data. Each event in these analyses is divided into two hemispheres and tagging is applied to each hemisphere independently. The efficiency is derived from the ratio of the events tagged on both sides to the number of tagged single hemispheres. The dominant systematic errors of the double-tag measurements are from the uncertainties in the estimation of the residual backgrounds and the correlation between tagging efficiencies in the two hemispheres.

The results of different measurements of R_b and R_c are presented in figures 12,13, respectively. They comprise the results obtained with the lepton, event-shape and lifetime b-quark tags, and lepton and various D-meson tagging of c-quarks.

At present the most precise results on R_b are from the combined lifetime and lepton double-tag measurements performed by ALEPH, DELPHI, OPAL and SLD.

Total relative error of the combined result of the R_b measurement is $\sim$ 0.7%, this measurement is systematics limited. A dominant systematic errors of the R_b measurement come from the uncertainties in the production fractions and decay multiplicities of different c-hadrons. These uncertainties could be reduced with further analyses of the LEP data, which are now competitive in precision with the data from lower energies.

Total relative error of the combined result of the R_c measurement is $\sim$ 5%, about-half of this error is systematics common between different experiments. The source of this common error is in the uncertainties of the charm production and branching fractions.

The measurements of the b- and c-quark forward-backward asymmetries are presented in tables 7,8. For the charge determination in these measurements the charge of the lepton in lepton tags, jet charge algorithms in lifetime tags and a $D^{*\pm}$-meson reconstruction analyses were used.

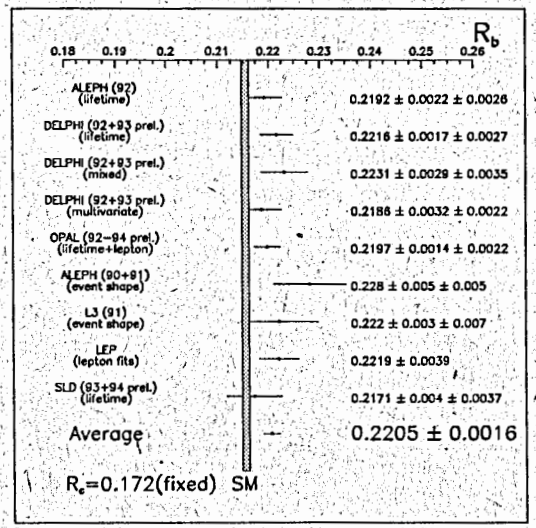

Figure 12: R_b measurement. The Standard Model prediction is for m_t=180±20 GeV.

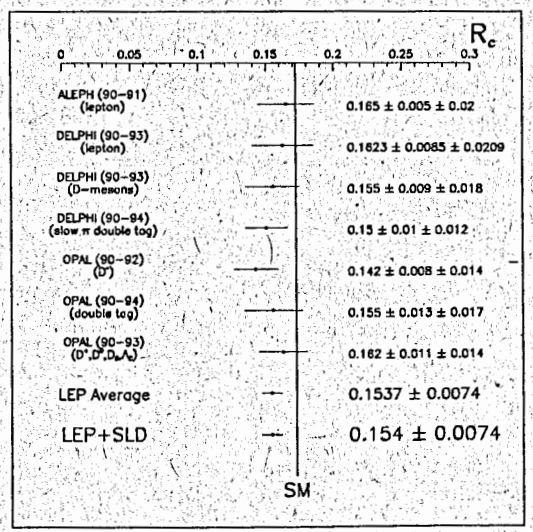

Figure 13: R_c measurement. The Standard Model prediction is for m_t=180±20 GeV.

For the consistent treatment of different results on b- and c-quark asymmetries several small corrections were applied, where necessary, to produce the pole asymmetries, $A_{FB}^{0,b}$ and $A_{FB}^{0,c}$.

Table 7: Results on b-quark forward-backward asymmetry measurements.

ALEPH(lept.)	90-93	$0.0846 \pm 0.0068 \pm 0.0022$
DELPHI(lept.)	91-94 prel.	$0.1049 \pm 0.0076 \pm 0.0035$
L3(lept.)	90-93 prel.	$0.103 \pm 0.010 \pm 0.004$
OPAL(lept.)	90-94 prel.	$0.1030 \pm 0.0090 \pm 0.0040$
ALEPH(jetc.)	90-93	$0.0992 \pm 0.0084 \pm 0.0047$
DELPHI(jetc.)	91-94 prel.	$0.0999 \pm 0.0072 \pm 0.0038$
OPAL(jetc.)	91-94 prel.	$0.0963 \pm 0.0067 \pm 0.0038$

Table 8: Results on c-quark forward-backward asymmetry measurements.

ALEPH(lept.)	90-91	$0.099 \pm 0.020 \pm 0.018$
DELPHI(lept.)	91-94 prel.	$0.084 \pm 0.014 \pm 0.013$
L3(lept.)	90-93 prel.	$0.083 \pm 0.038 \pm 0.025$
OPAL(lept.)	90-94 prel.	$0.049 \pm 0.009 \pm 0.012$
ALEPH(D^*)	91-94 prel.	$0.064 \pm 0.013 \pm 0.004$
DELPHI(D^*)	91-94 prel.	$0.075 \pm 0.012 \pm 0.006$
OPAL(D^*)	90-94 prel.	$0.068 \pm 0.014 \pm 0.007$

The heavy flavour forward-backward asymmetry measurements are still statistically dominated, they could be improved with increased statistics.

In addition to the pole asymmetries $A_{FB}^{0,b}$ and $A_{FB}^{0,c}$, the energy dependence of the asymmetries was measured. The energy dependence of the b- and c-quark forward-backward asymmetries is shown in figure 14. It follows well the Standard Model prediction also shown in this figure.

For the combination of the heavy flavour electroweak results a special procedure was developed by a LEP/SLD working group [13]. It allows for an account of common systematic errors and interdependence of parameters measured in the analyses simultaneously. The combination was performed as a multiparameter fit to the input data, which were individual results with the detailed breakdown of systematic errors and correlations. The fitted electroweak parameters were: R_b, R_c, $A_{FB}^{0,b}$, $A_{FB}^{0,c}$, $\mathcal{A}_b$ and $\mathcal{A}_c$. The latter two were introduced to parameterize the LEP forward-backward and the SLD polarized forward-backward asymmetries simultaneously without assumptions on $\mathcal{A}_e$.

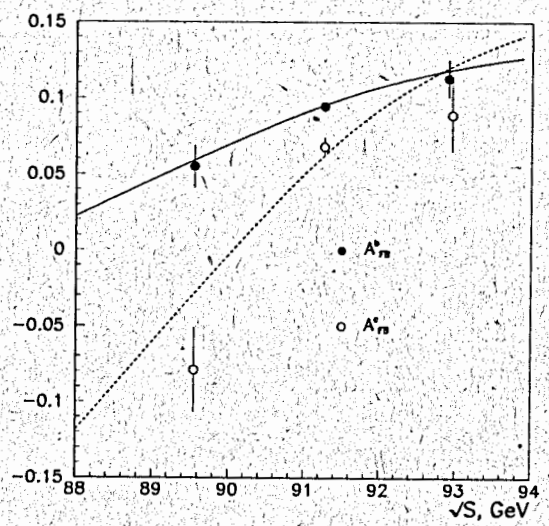

Figure 14: Energy dependence of the b- and c-quark forward-backward asymmetries.

Table 9: Electroweak results from heavy quarks.

R_b	0.2219 ± 0.0017
R_c	0.1540 ± 0.0074
$A_{FB}^{0,b}$	0.0997 ± 0.0031
$A_{FB}^{0,c}$	0.0729 ± 0.0058
$\mathcal{A}_b$	0.841 ± 0.053
$\mathcal{A}_c$	0.606 ± 0.090

The fitted values of the parameters are presented in table 9. Values of R_b and R_c were already given in figures 12,13 as the results of averaging. In these figures one can notice poor agreement with the Standard Model, the value of R_b is above, and R_c below the SM prediction.

There is a significant correlation ($\sim -35\%$) between these two measurements. Confidence level contours in $R_c - R_b$ plane are shown in figure 15.

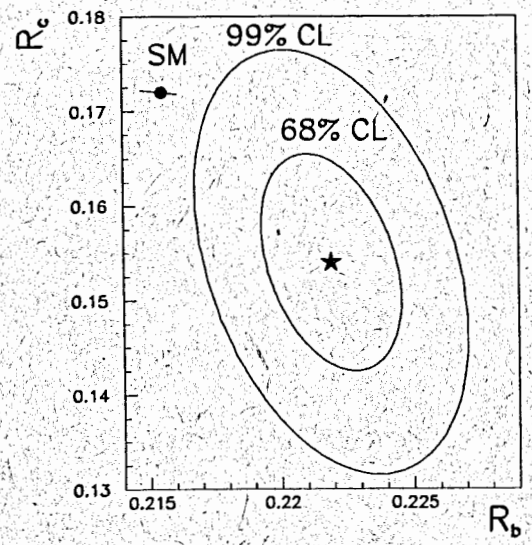

Figure 15: Contour plot of R_c versus R_b measurement. The Standard Model prediction is for m_t=180±20 GeV.

If R_c is fixed to its Standard Model prediction of 0.172, then the result for R_b is:

$$R_b(R_c = 0.172) = 0.2205 \pm 0.0016 \qquad (16)$$

The values of b- and c-quark pole asymmetries, $A_{FB}^{0,b}$ and $A_{FB}^{0,c}$, are less correlated and agree rather well with the Standard Model expectation (figure 16). Figure 17 shows the comparison of the direct measurements of the coupling parameters $\mathcal{A}_e$ and $\mathcal{A}_b$ performed by SLD with their product measured at LEP.

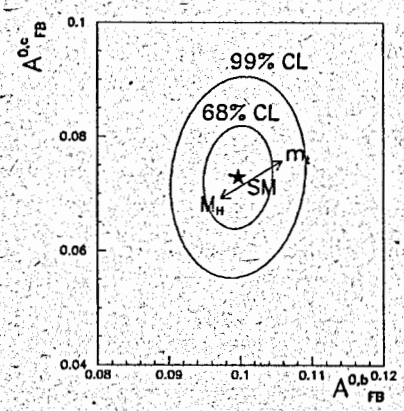

Figure 16: Contour plot of $A_{FB}^{0,c}$ versus $A_{FB}^{0,b}$ measurement. The Standard Model prediction is for m_t=180±20 GeV.

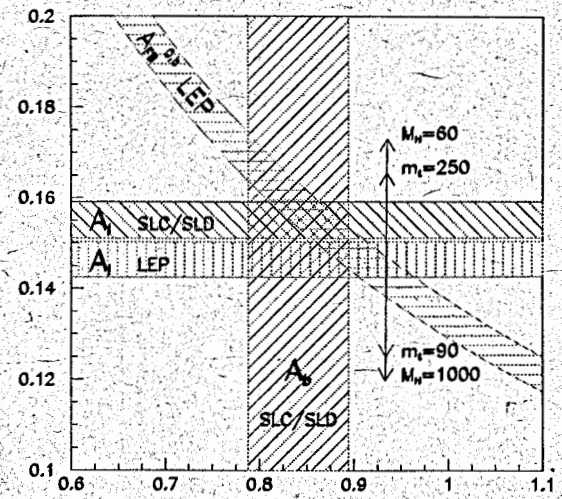

Figure 17: $\mathcal{A}_\ell$ versus $\mathcal{A}_b$ from different LEP and SLC measurements.

7 Measurement of the M_W

At present the most precise results of the W-boson mass measurements are from the analyses of leptonic decays of W's, produced at hadron colliders. In particular, recent results are from CDF and D0 experiments operating at FNAL Tevatron collider with the centre-of-mass energy of 1.8 TeV.

In the CDF analysis the W decays into both $e\nu$- and $\mu\nu$-channels were used. This published analysis, based on $\sim$ 19 pb^{-1} data sample, gives:

$$M_W = 80.410 \pm 0.180 \text{ GeV}, \tag{17}$$

as a combined result for both decay modes.

The D0 Collaboration has reported in 1994 a preliminary result:

$$M_W = 79.86 \pm 0.40 \text{ GeV}, \tag{18}$$

for the $e\nu$-channel, based on $\sim$ 13 pb^{-1}.

These two measurements, combined with older CDF and UA2 results, give:

$$M_W = 80.26 \pm 0.16 \text{ GeV}, \tag{19}$$

as the present world average for the direct measurement of the W-boson mass [14, 15]. In deriving this number a common systematic error of 85 MeV due to the uncertainties in the proton structure functions was used.

With the increased statistics at the Tevatron and with LEP operation at higher energies (above the WW-production threshold) there are distinct perspectives to improve the measurement of M_W to the level of $\sim$ 50 MeV or even below.

Recent measurements of the e^-p and e^+p cross section performed at HERA also show a sensitivity to the W propagator effects.

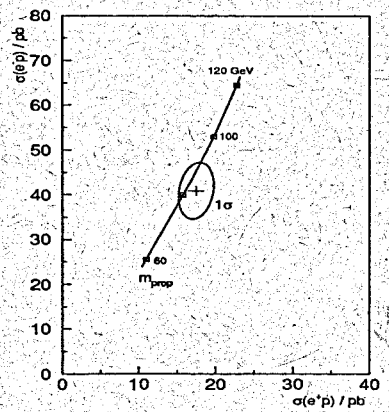

Figure 18: Measurement of the propagator effects at HERA.

This is illustrated in figure 18 as a 1σ (39% probability) contour plot of the combined H1/ZEUS measurement [16] compared to the Standard Model prediction for different masses of M_W.

8 Summary of electroweak measurements

The precise electroweak measurements discussed above are summarized in table 10.[1]

The results on $\sin^2\theta^{lept}_{eff}$ extracted from different asymmetry measurements presented in this table are shown in figure 19.

One can notice three classes of asymmetry measurements leading to about the same precision of 0.0005 in $\sin^2\theta^{lept}_{eff}$: combined LEP measurement of the lepton forward-backward asymmetries and τ-polarization, combined LEP measurement of the b-quark forward-backward asymmetry and the left-right asymmetry measured by SLD at SLAC.

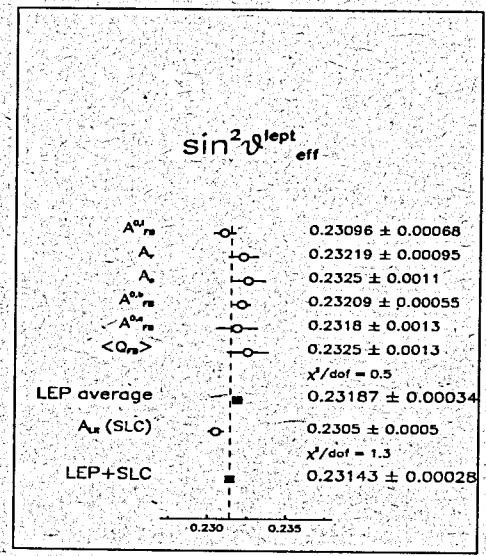

Figure 19: The results on the effective electroweak mixing angle.

All together these measurements provide an impressively precise determination of the $\sin^2\theta^{lept}_{eff}$ at the level of 0.00028.

The sensitivity of individual electroweak measurements from table 10 could be compared in terms of the indirect constraints which they provide on the top-quark mass, m_t.

This comparison is shown in figure 20, where m_t values were extracted from each single measurement using the constraints on M_Z, $\alpha_s(M_Z^2)$, $\alpha(M_Z^2)$ and M_H.

[1] For the determination of $1 - M_W^2/M_Z^2$ from the νN-scattering data see [17]

Table 10: Summary of electroweak measurements

	Experimental Measurement	Standard Model	Pull
LEP			
M_Z [GeV]	91.1884 ± 0.0022	91.1882	0.1
Γ_Z [GeV]	2.4963 ± 0.0032	2.4973	-0.3
σ_h^0 [nb]	41.488 ± 0.078	41.450	0.5
R_ℓ	20.788 ± 0.032	20.773	0.5
$A_{FB}^{0,\ell}$	0.0172 ± 0.0012	0.0159	1.1
$\mathcal{A}_\tau$	0.1418 ± 0.0075	0.1455	-0.5
$\mathcal{A}_e$	0.1390 ± 0.0089	0.1455	-0.7
R_b	0.2219 ± 0.0017	0.2156	3.7
R_c	0.1543 ± 0.0074	0.1724	-2.5
$A_{FB}^{0,b}$	0.0999 ± 0.0031	0.1020	-0.7
$A_{FB}^{0,c}$	0.0725 ± 0.0058	0.0728	0.0
$\sin^2\theta_{eff}^{lept}$			
from $\langle Q_{FB} \rangle$	0.2325 ± 0.0013	0.23172	0.6
SLD			
$\sin^2\theta_{eff}^{lept}$			
from A_{LR}	0.23049 ± 0.00050	0.23172	-2.5
R_b	0.2171 ± 0.0054	0.2156	0.3
$\mathcal{A}_b$	0.841 ± 0.053	0.935	-1.8
$\mathcal{A}_c$	0.606 ± 0.090	0.667	-0.7
$p\bar{p}$ and νN			
M_W [GeV]	80.26 ± 0.16	80.35	-0.5
$1 - M_W^2/M_Z^2$	0.2257 ± 0.0047	0.2237	0.4

In addition to the already mentioned precisely determined asymmetries, which constrain well the m_t, one can notice from this figure an important role of the precision Γ_Z measurement.

Indirect constraints on m_t compare well with the direct CDF/D0 measurement.

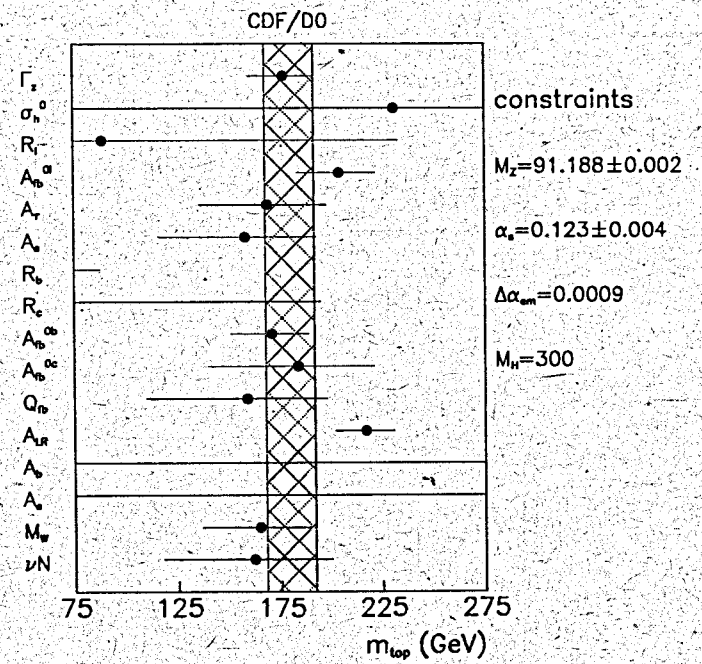

Figure 20: Sensitivity of different electroweak observables to m_t. The weighted average, $m_t = 180 \pm 12$ GeV, of the direct measurements by CDF and D0 is shown as a band.

9 Results and conclusions

The data from table 10 were used as an input to the global electroweak fit to determine the Standard Model parameters m_t and α_s. The results are presented in the upper part of table 11 and in figure 21. The central values of the fitted parameters are given for $M_H = 300$ GeV and the second error corresponds to the variation of M_H from 60 to 1000 GeV.

In this analysis the most up-to-date Standard Model calculations were used [18].

Table 11: Results of fit to the electroweak precision data for m_t and $\alpha_s(M_Z^2)$.

	LEP	LEP + SLD	LEP + SLD + $p\bar{p}$ and νN data
m_t (GeV)	$170 \pm 10\ ^{+17}_{-19}$	$180\ ^{+8}_{-9}\ ^{+17}_{-20}$	$178 \pm 8\ ^{+17}_{-20}$
$\alpha_s(M_Z^2)$	$0.125 \pm 0.004 \pm 0.002$	$0.123 \pm 0.004 \pm 0.002$	$0.123 \pm 0.004 \pm 0.002$
χ^2/d.o.f.	18/9	28/12	28/14
$\sin^2\theta^{lept}_{eff}$	$0.23206 \pm 0.00028\ ^{+0.00008}_{-0.00017}$	$0.23166 \pm 0.00025\ ^{+0.00006}_{-0.00013}$	$0.23172 \pm 0.00024\ ^{+0.00007}_{-0.00014}$
$1 - M_W^2/M_Z^2$	$0.2247 \pm 0.0010\ ^{+0.0004}_{-0.0002}$	$0.2234 \pm 0.0009\ ^{+0.0005}_{-0.0002}$	$0.2237 \pm 0.0009\ ^{+0.0004}_{-0.0002}$
M_W (GeV)	$80.295 \pm 0.057\ ^{+0.011}_{-0.019}$	$80.359 \pm 0.051\ ^{+0.013}_{-0.024}$	$80.346 \pm 0.046\ ^{+0.012}_{-0.021}$

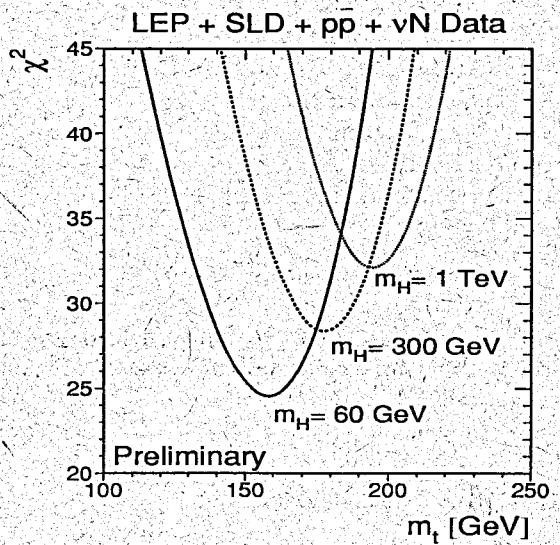

Figure 21: The χ^2 curves for the Standard Model fit of electroweak data.

Theoretical uncertainties in the interpretation of the data are at present dominated by the uncertainty in the value of the fine structure constant, $\alpha(M_Z^2)$. For the results presented in this report the value of $(\alpha(M_Z^2))^{-1} = 128.896 \pm 0.090$ was used [19, 20]. This uncertainty propagates into the uncertainty on the $\sin^2\theta^{lept}_{eff}$ prediction of 0.00025 or 4 GeV in terms of m_t, which was accounted for in the fit procedure.

The bottom part of the table contains results for $\sin^2\theta^{lept}_{eff}$, $1 - M_W^2/M_Z^2$ and M_W derived from the fitted parameters.

The χ^2 values of the fits repeated with different sets of data have poor probabilities (0.6-3.5%), which is almost exclusively due to the deviations observed for R_b and R_c.

To study the influence of these particular data on the Standard Model parameters determination, the fit was repeated excluding R_b and R_c measurements from the input. As a result the m_t value increases by 4 GeV and the value of $\alpha_s(M_Z^2)$ stays approximately constant.

The fitted value of m_t is in excellent agreement with the result of the direct measurement of the top-quark mass by CDF [21] ($m_t = 176 \pm 8 \pm 10$ GeV) and D0 [22] ($m_t = 199^{+19}_{-21} \pm 22$ GeV) at the TEVATRON.

The value of $\alpha_s(M_Z^2)$ derived from the fit of precision electroweak data agrees well with that obtained from event-shape measurements at LEP, $\alpha_s(M_Z^2) = 0.123 \pm 0.006$.

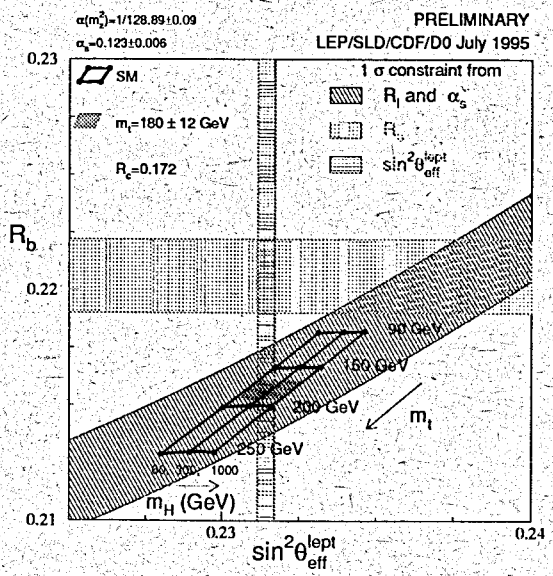

Figure 22: The measurements of $\sin^2\theta^{lept}_{eff}$ and R_b. Also shown is the constraint resulting from the measurement of R_ℓ, assuming $\alpha_s(M_Z^2) = 0.123 \pm 0.006$.

This value depends, however, on the interpretation given to the deviation of R_b and R_c. For example, if the fit is repeated propagating the observed deviation in b-quark partial width ($11.7 \pm 3.8 \pm 1.4$ MeV) into Γ_{had}, which is measured independently, the result is $\alpha_s(M_Z^2) = 0.102 \pm 0.008$ and the value of m_t increases by 3 GeV only.

This is illustrated in figure 22 where the constraints from the measurements of $\sin^2\theta^{lept}_{eff}$, R_b, R_ℓ and $\alpha_s(M_Z^2)$ are shown.

The change in the χ^2 minima for the fits with different masses of the Higgs-boson in figure 21 suggests that some information on M_H could be extracted from the analysis of precision electroweak data. One would expect, however, the present constraint on M_H to be rather weak because the main M_H dependences of the Standard Model predictions for electroweak observables are logarithmic and the effects of M_H and m_t are correlated. The results of the fit to the electroweak data, which include also combined CDF/D0 result ($m_t = 180 \pm 12$ GeV), are presented in figure 23. The minima of the χ^2 of the fits occur at low values of M_H (below 100 GeV for the data including R_b and R_c).

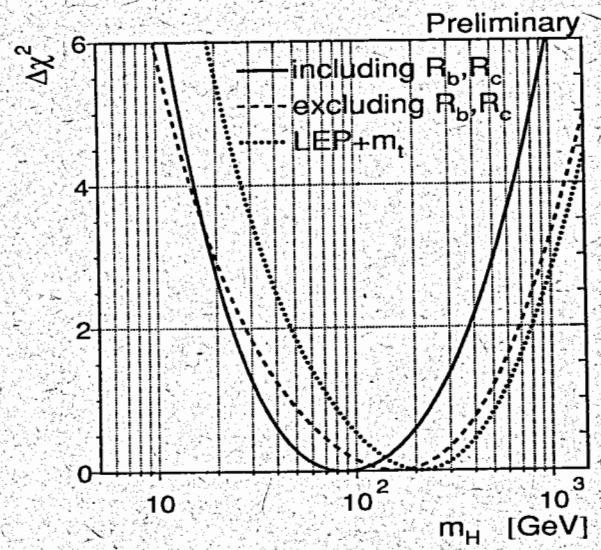

Figure 23: The $\Delta\chi^2$ curves for the fits with M_H free.

The range up to $\sim$ 600 GeV is accommodated within the 95% confidence level interval. When R_b and R_c or A_{LR} measurements are excluded from the fit the position of the minimum is shifted towards higher values of M_H.

In conclusion:

Recent electroweak results significantly increased the precision of our tests of the Standard Model.

An indirect determination of the m_t established by the global fit to the electroweak observables shows very good agreement with the direct measurement of the top-quark mass.

The large χ^2 of the global fits is almost exclusively due to the deviations in R_b- and R_c-measurements. These measurements are largely dominated by systematics and need further experimental studies, in particular, on the production and fragmentation of c-hadrons.

The present data show weak sensitivity to M_H, low M_H values are slightly preferred. Better sensitivity is expected with the new measurements in quark sector, $\sin^2\theta^{lept}_{eff}$, M_W and m_t.

Acknowledgements

I would like to thank all my colleagues and, in particular, experiment representatives for providing me with their results and for many interesting discussions and help.

Cordial thanks are owed to the members of the LEP Electroweak Working Group, the work in this group was essential in the preparing of my talk.

My special thanks go to organizers of this excellent conference both for their invitation and hospitality.

References

[1] R. Assmann et al., *Zeit. Phys.* **C66** (1995) 567.

[2] S. Jadach et al., *Phys. Lett.* **B353** (1995) 362.

[3] The LEP Collaborations and the LEP Electroweak Working Group, CERN-PPE/95-172.

[4] LEP Electroweak Working Group, Internal Note LEPEWWG/LS/95-01.

[5] DELPHI Collaboration, eps0521. L3 Collaboration, eps0113.

[6] M. Woods, Proceedings of the International Conference on High Energy Physics, Brussels 1995.

[7] R. St Denis, Proceedings of the International Conference on High Energy Physics, Brussels 1995.

[8] D. Charlton, Proceedings of the International Conference on High Energy Physics, Brussels 1995.

[9] T. Behnke, Proceedings of the International Conference on High Energy Physics, Brussels 1995.

[10] A. Passeri, Proceedings of the International Conference on High Energy Physics, Brussels 1995.

[11] SLD Collaboration, eps0222.

[12] J. Huber, Proceedings of the International Conference on High Energy Physics, Brussels 1995.

[13] The LEP and SLD Heavy Flavour Working Groups, Internal Note LEPHF/95-02.

[14] L. Nodulman, Proceedings of the International Conference on High Energy Physics, Brussels 1995.

[15] M. Demarteau et al., CDF 2552 and D0NOTE 2115.

[16] H1 Collaboration, DESY 95-102. ZEUS Collaboration, DESY 95-053.

[17] D.Harris, Proceedings of the International Conference on High Energy Physics, Brussels 1995.

[18] Eds. D. Bardin, W. Hollik and G. Passarino, CERN Yellow Report 95-03.

[19] S. Eidelmann and F. Jegerlehner, *Zeit. Phys.* **C67** (1995) 585.

[20] H. Burkhardt and B. Pietrzyk, *Phys. Lett.* **B356** (1995) 398.

[21] CDF Collaboration, F. Abe et al., *Phys. Rev. Lett.* **74** (1995) 2626.

[22] D0 Collaboration, S. Abachi et al., *Phys. Rev. Lett.* **74** (1995) 2632.

Received by Publishing Department
on February 12, 1996.

Ольшевский А.Г. E1-96-45

Прецизионная проверка стандартной модели

Приведены и обсуждаются результаты современных прецизионных измерений величин, предсказываемых в стандартной модели объединения электромагнитного и слабого взаимодействий. Совокупность этих измерений служит экспериментальной основой, позволяющей проверить принципы и определить параметры стандартной модели на новом высоком уровне точности.

Работа выполнена в Лаборатории ядерных проблем ОИЯИ.

Препринт Объединенного института ядерных исследований. Дубна, 1996

Olchevski A.G. E1-96-45

Precision Tests of the Standard Model

The present status of the precision measurements of electroweak observables is discussed with the special emphasis on the results obtained recently. All together these measurements provide the basis for the stringent test of the Standard Model and determination of the SM parameters.

The investigation has been performed at the Laboratory of Nuclear Problems, JINR.

Preprint of the Joint Institute for Nuclear Research. Dubna, 1996